Understanding gold toxicity in aerobically-grown *Escherichia coli*

C. Muñoz-Villagrán[1], F. Contreras[1], F. Cornejo[1], M. Figueroa[1], D. Valenzuela-Bezanilla[2], R. Luraschi[1], C. Reinoso[2], J. Rivas-Pardo[1,3], C. Vásquez[1], M. Castro[2]* and F. Arenas[1]*

Abstract

Background: There is an emerging field to put into practice new strategies for developing molecules with antimicrobial properties. In this line, several metals and metalloids are currently being used for these purposes, although their cellular effect(s) or target(s) in a particular organism are still unknown. Here we aimed to investigate and analyze Au^{3+} toxicity through a combination of biochemical and molecular approaches.

Results: We found that Au^{3+} triggers a major oxidative unbalance in *Escherichia coli*, characterized by decreased intracellular thiol levels, increased superoxide concentration, as well as by an augmented production of the antioxidant enzymes superoxide dismutase and catalase. Because ROS production is, in some cases, associated with metal reduction and the concomitant generation of gold-containing nanostructures (AuNS), this possibility was evaluated in vivo and in vitro.

Conclusions: Au^{3+} is toxic for *E. coli* because it triggers an unbalance of the bacterium's oxidative status. This was demonstrated by using oxidative stress dyes and antioxidant chemicals as well as gene reporters, RSH concentrations and AuNS generation.

Keywords: Gold(III), Toxicity, Resistance, *E. coli*, Aerobic, Anaerobic

Background

In addition to carbon, hydrogen, oxygen, and nitrogen, biomolecules are made of a number of other elements such as iron, calcium and magnesium, among others [1]. Some of them are critical for several biochemical processes and form part of the cell membrane, nucleic acids as well as protein structure [2]. Metals like iron are so fundamental for life that they are often referred to as essential [3]. The list of essential elements includes also Na, Mg, K, Ca, V, Cr, Mn, Fe, Co, Ni, Cu, Zn, Se and Mo [2]. On the other hand, non-essential metals—i.e., those that do not display known biological roles in living organisms—, include Ag, Hg, Te, and Au [2], and are actually extremely toxic for microorganisms [1].

Given their toxicity, a number of these non-essential metals are currently being used as antimicrobial compounds by incorporating them on surfaces and coatings medical and pharmaceutical equipment [4]. Particularly, and since silver, gold, copper and titanium exhibit physicochemical characteristics favoring their antimicrobial activity, they are nowadays usually included in several nanomaterials [5]. The toxicity of some metals and metalloids such as chromate and tellurite is related to the generation of reactive oxygen species (ROS) [6–10], which then damage key cell components and affect bacterial growth [11].

Gold (III) is toxic for *E. coli*, displaying a minimal inhibitory concentration (MIC) around 20 µM, twice

*Correspondence: miguelcastro@santotomas.cl; felipe.arenass@usach.cl
[1] Laboratorio Microbiología Molecular, Departamento de Biología, Facultad de Química y Biología, Universidad de Santiago de Chile, Santiago, Chile
[2] Laboratorio de Microbiología Aplicada, Departamento de Ciencias Básicas, Facultad de Ciencias, Universidad Santo Tomás, Sede Santiago, Chile
Full list of author information is available at the end of the article

Muñoz-Villagrán *et al. Biol Res*   (2020) 53:26

Page 2 of 9

that of the extremely toxic Hg(I) [1]. In a more recent article, Nam and coworkers showed that Au^{3+} altered significantly the growth of *E. coli*, *Bacillus subtilis* and other aquatic microorganisms [12]. Although the specific mechanism of gold toxicity for *E. coli* has not been elucidated yet, given that Au^{3+} belongs to the group of soft metal ions [13], it is probable that it interacts with soft bases such as thiols and/or other cell targets containing soft base groups [2]. Since one of the main reduced thiol targets is glutathione (GSH) [13], Au^{3+} uptake could generate an intracellular redox unbalance that ultimately affects the viability of the microorganism [14]. Transcriptomic microarray experiments were conducted to assess the response of *Cupriavidus metallidurans* CH34 to aqueous Au(III)-complexes which appear to be toxic because they become oxidative once inside the cell [15, 16].

Currently, nanostructures (NS) containing some of these non-essential metals are used in diverse applications such as water treatment, photocatalysis, optics and therapeutic procedures, among others [5, 17]. In particular, gold nanostructures (AuNS) behave as potent antimicrobial agents against multidrug resistant Gram-negative and Gram-positive bacteria [18]. In general, it has been suggested that AuNS would be toxic because they can generate ROS, similar to that seen in many other antibacterial materials such as ZnO, TiO_2 and Ag nanoparticles (NPs) [17, 19, 20]. Other targets depend on the route of gold(III) complexes synthesis or composition; for instance, AuNPs covered with organic molecules such as 4,6-diamino-2-pyrimidinethiol produce i) a change in membrane potential that limits ATPase activity and ii) inhibit tRNA binding to the ribosome, thus leading to a collapse of several biological processes without ROS production [21]. In
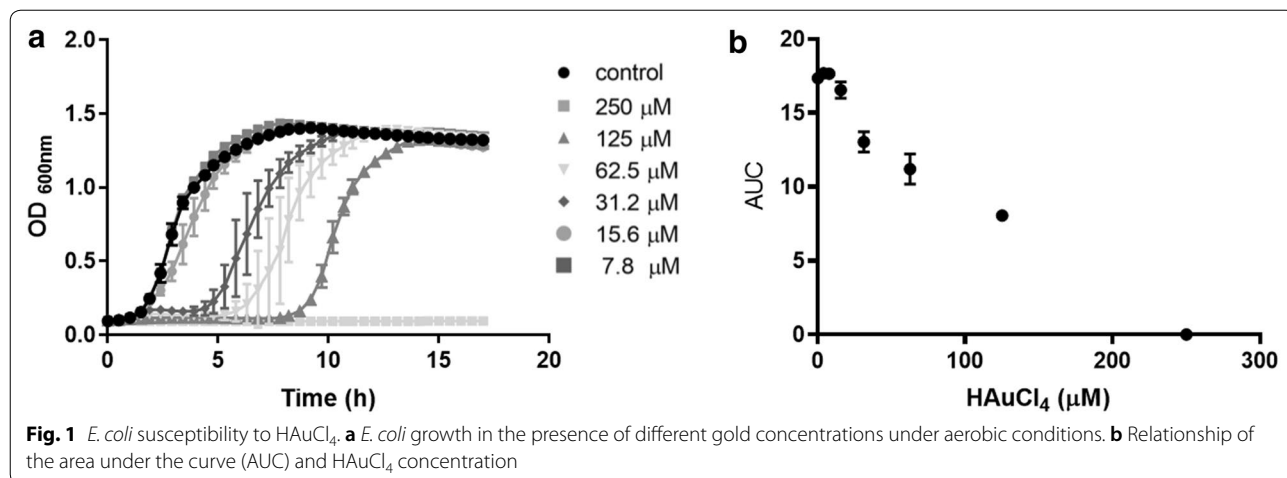
spite of this evidence, specific mechanism(s) by which Au^{3+} triggers cell toxicity are still unanswered.

In this work, we aimed to shed light on Au^{3+} antimicrobial activity. By combining ROS-sensitive probes, oxygen scavengers, transcriptional induction analysis and intracellular thiol concentration determinations, we found that *E. coli* exposure to Au^{3+} results in the generation of an oxidative unbalance characterized by increased ROS levels, overproduction of antioxidant enzymes, decreased levels of reduced thiols, and in vivo and in vitro generation of AuNS. These findings represent an initial attempt to elucidate the molecular basis of bacterial Au^{3+} toxicity.

Results

A number of tests including susceptibility assays, growth curves, growth inhibition areas and MIC were used to characterize the toxicity triggered by Au^{3+} in *E. coli*. Under aerobic conditions, the Au^{3+} MIC was 250 μM and growth inhibition area was 1.12 ± 0.02 cm². Negligible effects on cell growth were observed when *E. coli* was exposed to lower Au^{3+} concentrations (7.8–15.6 μM). Nevertheless, when the metal concentration was raised to 31.2–125 μM, the lag phase was extended compared to that exhibited by untreated controls. No growth was observed at Au^{3+} concentrations above 250 μM (Fig. 1a). To assess the impact of the metal on *E. coli* growth, the Area Under Curve (AUC) of the growth curve at each concentration tested was calculated. Figure 1b shows a dose–response relationship between $HAuCl_4$ concentration and AUC, indicating that at Au^{3+} concentrations above 250 μM growth is severely inhibited.

We hypothesized that the initial lag observed with $HAuCl_4$ above 15.6 μM and below 250 μM could be due to the establishment of an oxidative stress status, a phenomenon well documented for other metal(loid)s [8, 22, 23]. Then, cell viability was determined in the presence of

Fig. 1 *E. coli* susceptibility to $HAuCl_4$. **a** *E. coli* growth in the presence of different gold concentrations under aerobic conditions. **b** Relationship of the area under the curve (AUC) and $HAuCl_4$ concentration

Muñoz-Villagrán *et al. Biol Res*   (2020) 53:26

Page 3 of 9

two ROS scavengers: ascorbic acid [24] and 2,2′-Bipyridyl (iron chelator that prevents hydroxyl radical production) [25]. Figure 2 shows the effect of both scavengers on cells exposed to 200 μM $HAuCl_4$. The presence of either ascorbate or 2,2′-Bipyridyl reverted, although not completely, the toxic effects of Au^{3+} regarding untreated controls. These results suggest that, at least in part, Au^{3+} toxicity is ROS-mediated.

ROS generation by $HAuCl_4$ was assessed using the fluorescent probes H_2DCFDA and DHE, which allow determining total ROS and superoxide, respectively. Figure 3 shows ROS formation in *E. coli* exposed to $HAuCl_4$ under aerobic and anaerobic conditions. Tellurite-mediated ROS generation [8, 26] was included for comparison. As expected, total ROS as well as superoxide levels increased with increasing Au^{3+} concentrations (Fig. 3a, c). In turn, no changes were detected in the absence of oxygen (Fig. 3b, d). The probe altogether with the metal did not generate increased fluorescence (cell-free control, not shown).

Given that Au^{3+} exposure results in increased ROS levels, a transcriptional response was also expected. Such response was investigated using *E. coli* strains GS022 and SP11, which contain the *lacZ* gene downstream the promoters of *katG* and *soxS* genes, respectively [27]. Figure 4 shows that the reporter activity increases upon exposure to 200 μM $HAuCl_4$, a change that was observed only under aerobic conditions. The highest induction (200-fold) was observed in SP11 cells (Fig. 4b), while the *katG*::*lacZ* construct was induced only three fold regarding untreated controls (Fig. 4a). Taken together, these

results allow speculating that enzymes such as catalase, peroxidase, superoxide dismutase and probably glucose-6-phosphate dehydrogenase are overproduced in response to $HAuCl_4$.

In general, oxidative stress alters the equilibrium among some cellular components; in this line, the thiol reactive dye DTNB was used to assess the intracellular redox unbalance triggered by the toxicant. Tellurite and menadione, two compounds previously shown to affect intracellular thiol (RSH) levels were used as positive controls [8]. As expected, tellurite caused a change in thiol levels only under aerobic conditions, while menadione decreased RSH levels both in aerobiosis and anaerobiosis. Au^{3+} treatment resulted in a dose-dependent decrease of the RSH pool (Fig. 5), a result that matchs our initial observations regarding $HAuCl_4$ toxicity in an oxygen-free environment (Additional file 1: Figure S1).

Finally, it was analyzed if $HAuCl_4$-mediated ROS generation in *E. coli* is accompanied by a concomitant generation of AuNS which eventually would decrease metal toxicity. Figure 6a shows that *E. coli* forms AuNSs that accumulate homogeneously within the bacteria in the presence of 1 mM gold (III). AuNSs were also synthesized in vitro using cell-free crude extract (Fig. 6b), which showed a spheroidal shape and an average size of 20–30 nm.
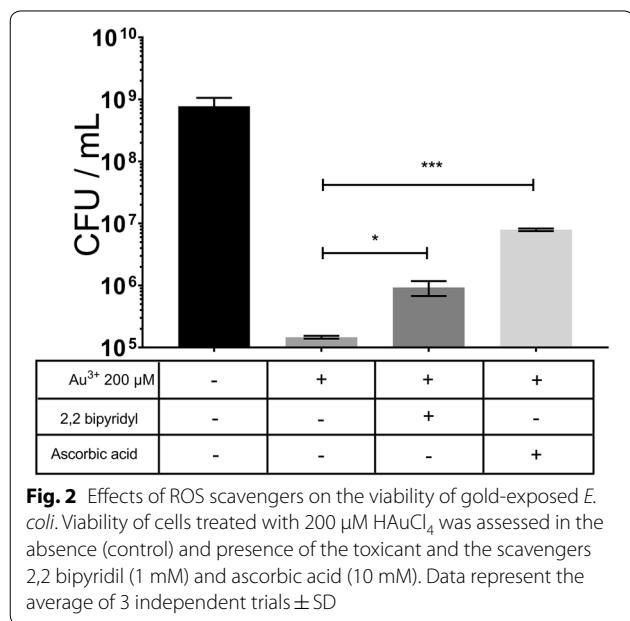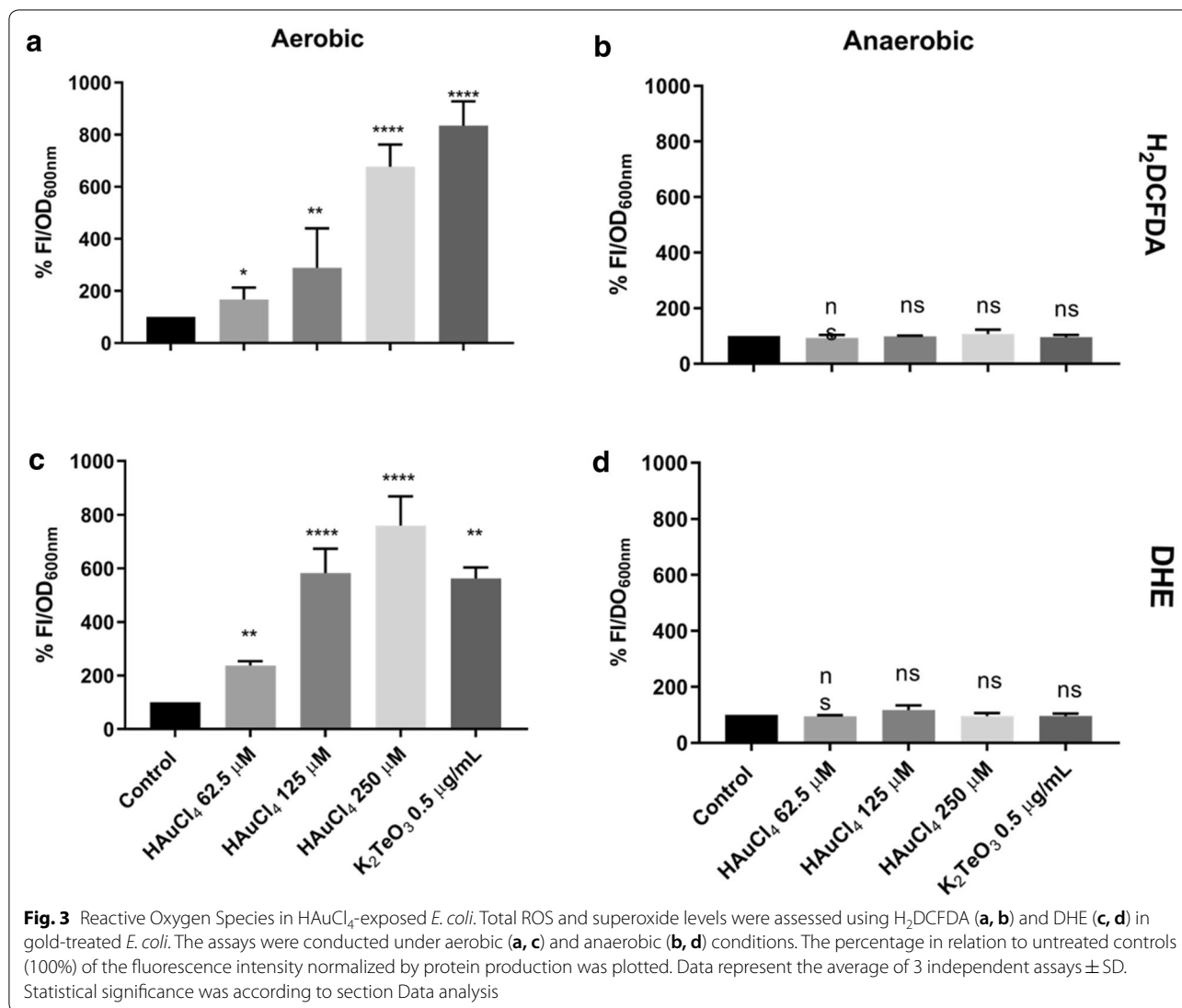
Discussion

Some metals are essential in trace amounts for the functioning of living organisms; however, most of them become toxic at higher concentrations [1]. Part of the toxicity exhibited by heavy metal cations such as Hg^+, Cd^+ and Ag^+ occurs mainly because of their trend to bind cellular thiol groups like glutathione, especially in Gram negative bacteria [28]. Nevertheless, it has been also shown that their toxicity is related to the generation of an oxidative stress status in the cell [2, 9], thus affecting other cell targets such as thiol content [29] and heme biosynthesis [30].

Although harmful effects of gold for microorganisms are partially known [1], detailed gold(III) toxicity studies are still scarce. Some examples include the synthesis of gold nanostructures, which are being currently used as antimicrobial agents [31] and in other biomedical applications [32, 33].

Susceptibility assays showed that gold effects on *E. coli* growth are proportional to metal concentration and that the lag phase was affected in the presence of 31–125 μM $HAuCl_4$ (Fig. 1a, b). The gold minimal inhibitory concentration for *E. coli* was 250 μM, where, as expected, a total inhibition of the bacterial growth was observed (Fig. 1).

Since several metals are toxic because of ROS production, oxidative damage generation upon gold exposure
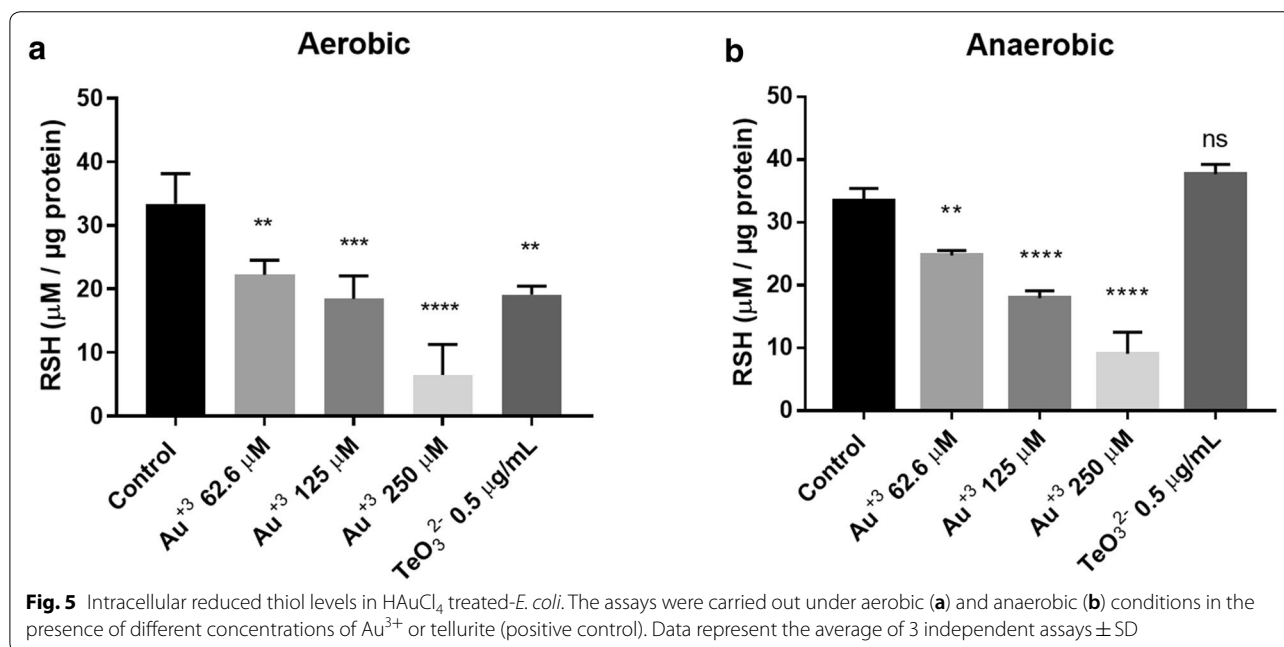
Fig. 2 Effects of ROS scavengers on the viability of gold-exposed *E. coli*. Viability of cells treated with 200 μM $HAuCl_4$ was assessed in the absence (control) and presence of the toxicant and the scavengers 2,2 bipyridil (1 mM) and ascorbic acid (10 mM). Data represent the average of 3 independent trials ± SD

Muñoz-Villagrán *et al. Biol Res*   (2020) 53:26

Page 4 of 9

Fig. 3 Reactive Oxygen Species in HAuCl$_4$-exposed *E. coli*. Total ROS and superoxide levels were assessed using H$_2$DCFDA (**a, b**) and DHE (**c, d**) in gold-treated *E. coli*. The assays were conducted under aerobic (**a, c**) and anaerobic (**b, d**) conditions. The percentage in relation to untreated controls (100%) of the fluorescence intensity normalized by protein production was plotted. Data represent the average of 3 independent assays ± SD. Statistical significance was according to section Data analysis
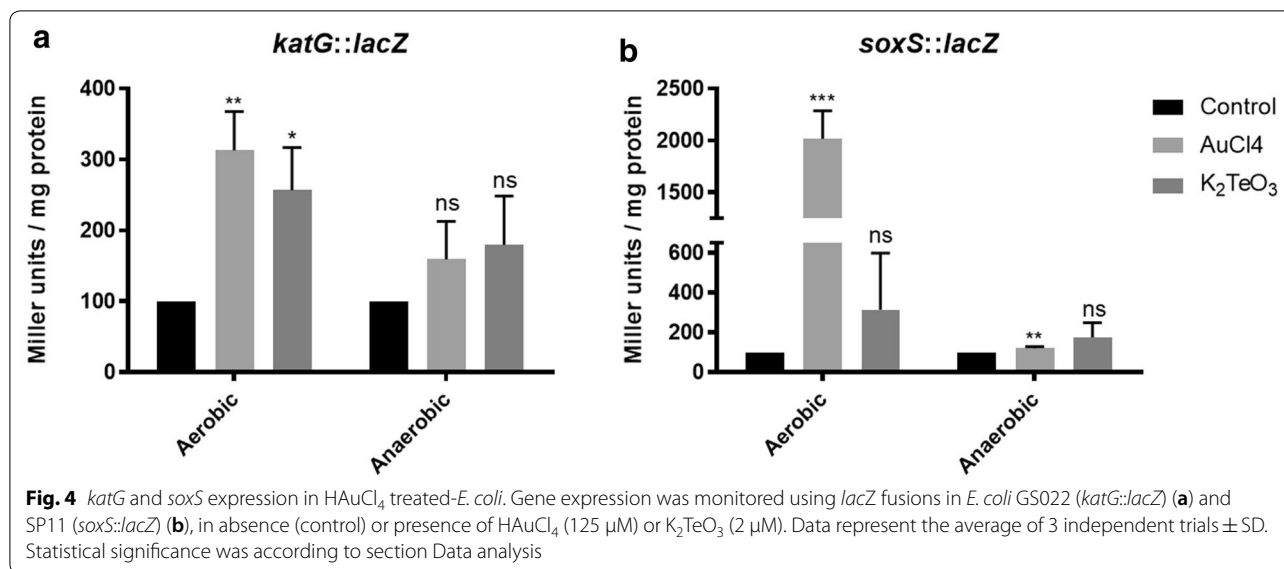
was evaluated under aerobic conditions in the presence of the ROS scavengers 2,2´-Bipyridyl and ascorbic acid [21]. Figure 2 shows that 2,2´-Bipyridyl improved significantly the growth of *E. coli* exposed to Au^{3+}, probably because of a decreased formation of hydroxyl radicals. Likewise, the presence of ascorbic acid favored *E. coli* growth by more than two log units. In this line, it has been shown that the low redox potential of ascorbate protects against increased metal-induced superoxide generation [34]. While ascorbic acid and 2,2´-Bipyridyl have been used as scavengers of ROS to evaluate the antioxidant effect of certain compounds, in other studies ascorbate is used as Au(III)-reducing agent and 2,2-Bipyridyl to synthesize nanoparticles [35, 36]. It is possible that there is an interaction of these molecules with Au(III), which would decrease metal bioavailability and therefore toxicity (Fig. 2). Formation of gold NS are carried out under

defined conditions, for example, high ascorbate concentrations allow rapid gold reduction at acid pH [35], which does not occur in our conditions. Furthermore, nanoparticles and bipyridyl form complexes that are adducts linked by coordination with HAuCl$_4$*3H$_2$O and derivatives of 6-benzyl-2,2′-Bypiridine in ethanol solution [37]. Then, to rule out the putative interaction between Au(III) and these antioxidant molecules, experiments were repeated adding this time a pre-incubation step of cells grown up to OD ~ 0.4 nm for 30 min; cells were then washed with fresh medium and treated with 0.2 mM Au(III) for 15 min. Results indicated that the antioxidants generate a protective effect against toxicant-generated ROS (Additional file 2: Figure S2).

On the other hand, ROS generation was assessed using the fluorescent probes H$_2$DCFDA and DHE, which detect total ROS [38] and superoxide [39], respectively. Cells

Muñoz-Villagrán *et al. Biol Res*   (2020) 53:26

Page 5 of 9

Fig. 4 *katG* and *soxS* expression in HAuCl₄ treated-*E. coli*. Gene expression was monitored using *lacZ* fusions in *E. coli* GS022 (*katG::lacZ*) (**a**) and SP11 (*soxS::lacZ*) (**b**), in absence (control) or presence of HAuCl₄ (125 μM) or K₂TeO₃ (2 μM). Data represent the average of 3 independent trials ± SD. Statistical significance was according to section Data analysis

Fig. 5 Intracellular reduced thiol levels in HAuCl₄ treated-*E. coli*. The assays were carried out under aerobic (**a**) and anaerobic (**b**) conditions in the presence of different concentrations of Au³⁺ or tellurite (positive control). Data represent the average of 3 independent assays ± SD

treated with Au^{3+} showed increased fluorescence that was proportional to toxicant concentration, thus indicating that Au(III) indirectly produces ROS (Fig. 3). However and as expected, this effect was only observed under aerobic conditions. Particularly, higher fluorescence was observed with the superoxide-detecting probe, suggesting that O_2^-· would be the main ROS generated by Au(III) in *E. coli* (Fig. 3c).

Because of the above results, the cell antioxidant response was evaluated. *E. coli* exposure to Au^{3+} also resulted in increased induction of *soxS* and *katG* genes in

aerobic conditions, (Fig. 4). Since SoxS activates a group of enzymes that mitigate the effects of superoxide [40], these results support the observation that Au^{3+} generate ROS. Peroxide formed from superoxide dismutation by the enzyme superoxide dismutase [41] is in turn decomposed to H_2O and O_2 by KatG, hydroperoxidase I (HPI) and/or catalase.

Since gold -like other soft metals- displays affinity for soft bases such as sulfhydryl groups [2] which could result in a redox unbalance [42], the effect of gold exposure on the level of cell RSH was evaluated. The level of
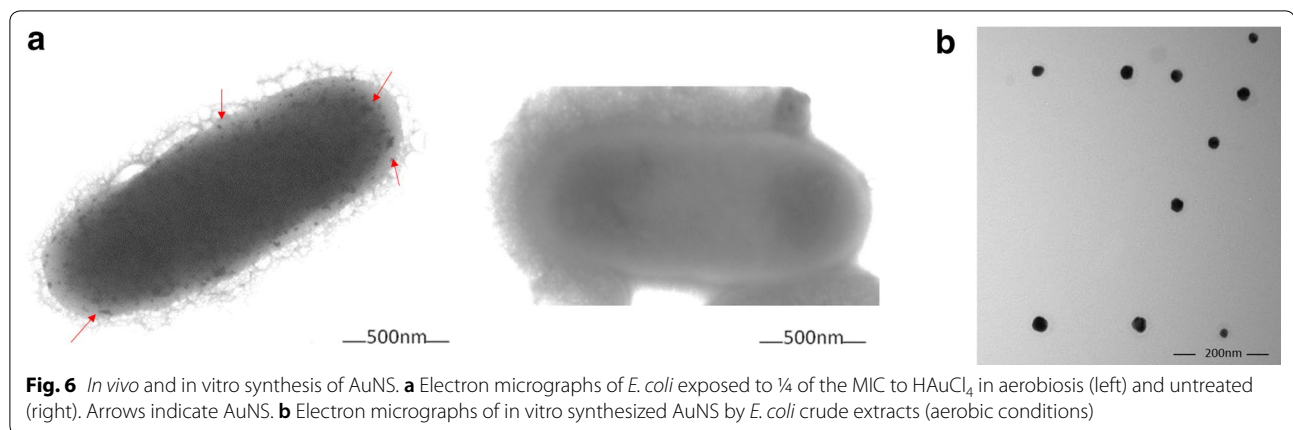
Muñoz-Villagrán *et al. Biol Res*   (2020) 53:26

Page 6 of 9

Fig. 6 *In vivo* and in vitro synthesis of AuNS. **a** Electron micrographs of *E. coli* exposed to ¼ of the MIC to HAuCl$_4$ in aerobiosis (left) and untreated (right). Arrows indicate AuNS. **b** Electron micrographs of in vitro synthesized AuNS by *E. coli* crude extracts (aerobic conditions)

reduced cellular thiols decreased upon gold treatment both in aerobic and anaerobic conditions (Fig. 4). Surprisingly, *E. coli* growth was more affected in the absence of oxygen (Additional file 1: Figure S1); although toxicity of this metal in this case is independent of ROS, it has also been described that it is still toxic in anoxic environments [43]. This interesting anaerobic effect is under investigation in our laboratory.

Finally, one of the putative mechanisms of bacterial response to metal(loid)s is their reduction to the respective elemental state, which has been widely studied [44–47]. Given that *E. coli* crude extracts were able of gold(III) reduction generating a characteristic red precipitate (not shown), the possibility of synthesizing AuNS in vivo and in vitro was explored (Fig. 6). *E. coli* formed AuNS which accumulated homogeneously inside cells, suggesting that AuNS formation by *E. coli* could be consequence of a series of metabolic events in response to HAuCl$_4$ exposure.

Conclusion

Au^{3+} is toxic for *E. coli* because it triggers an unbalance of the bacterium's oxidative status. This was demonstrated by using oxidative stress dyes and antioxidant chemicals as well as gene reporters, RSH concentrations and AuNS generation.

Methods
Strains and growth conditions

E. coli BW25113, SP11, and GS022 [27] used in this work were grown in LB medium [48] as previously described [49]. All procedures were carried out at 37 °C under aerobic and, eventually, anaerobic growth conditions. Cells were cultured in thermostabilized orbital shakers; oxygen deprived cultures were conducted inside an anaerobic chamber filled with 100% N$_2$ (Coy Lab Products). Inside

the Coy chamber a multimode plate reader TECAN equipment was available for anaerobic experiments.

Growth curves

Overnight cultures were diluted 1:100 with fresh LB medium and incubated in an orbital shaker to OD$_{600nm}$ ~ 0.6. Then, 10 µL were added to 1 mL of fresh LB medium containing different concentrations of HAuCl$_4$. Bacterial growth was monitored every 30 min at 600 nm for 18 h using a multimode plate reader (TECAN Infinite M200 Pro). The area under the curve (AUC) [50, 51] was calculated with the R package Growth Curver as described by Sprouffske and Wagner [52].

Determination of the minimal inhibitory concentration (MIC)

MIC determinations were carried out using serial dilutions (1:2) of a sterile solution of HAuCl$_4$ in LB medium in 48-well plates. Subsequently, 10 µL of cultures grown in LB medium to OD$_{600nm}$ ~ 0.6 were added to each well and incubation proceeded with constant shaking at 37 °C. MICs were determined after 24 h of incubation.

Determination of growth inhibition zones

Overnight cultures were diluted 1:100 with fresh LB medium and incubated with shaking to OD$_{600nm}$ ~ 0.6. After dilution to OD$_{600nm}$ ~ 0.1, 100 µL were evenly spread on agar LB-plates. After air drying, 10 µl of 50 mM HAuCl$_4$ were deposited on sterile filter disks placed on the centers of the plates as described by Contreras et al. [53]. Growth inhibition areas were determined after overnight incubation at 37 °C. To make a correct analysis of the absorbance data obtained in the TECAN plate reader and thus compare the effect on the doubling time, the load capacity and growth rate, the R Growth curver software was used [52]. The AUC (arbitrary unit) metric integrates the information of the parameters K

Muñoz-Villagrán *et al. Biol Res*   (2020) 53:26

Page 7 of 9

(maximum possible size of the population), r (intrinsic growth rate of the population) and N_0 (size of the population at the beginning of the curve). These parameters are useful to summarize and compare cell growth dynamics [52], and corroborated that toxicant concentration affects directly the bacterial population.

Cell viability

Overnight cultures grown in LB medium were diluted (1:100) to $OD_{600nm} \sim 0.4$. Then the following treatments were conducted: bacteria were grown in the absence or presence of 200 µM $HAuCl_4$, supplemented or not with 1 mM 2,2´-Bipyridyl or 10 mM ascorbic acid. Cultures were treated for 15 min and then serial dilutions were plated on LB/agar. CFU were determined after overnight incubation at 37 °C.

β-galactosidase assay

E. coli SP11 (*soxS::lacZ*) and GS022 (*katG::lacZ*) were used for stress-promoter activation assays as described by Arenas et al. [27]. Thirty ml of LB medium were inoculated with 300 µl of overnight cultures and grown at 37 °C under aerobic or anaerobic conditions to $OD_{600nm} \sim 0.4$. Aliquots of 6 mL were treated with $HAuCl_4$ (125 µM), K_2TeO_3 (2 µM) or without the toxicants for 30 (SP11) and 25 min (GS022), respectively. After incubating on ice for 15 min, OD_{600nm} was determined and cells were sedimented by centrifugation at $13,000 \times g$ for 3 min. Cell pellets were permeabilized with chloroform (1%) and sodium dodecyl sulfate (SDS 0.1%), and suspended in 1.5 mL of previously chilled buffer Z (40 mM Na_2HPO_4 H_2O; 60 mM NaH_2PO_4 7 H_2O, pH 7.5 that contained 10 mM KCl, 1 mM $MgSO_4$ and 50 mM β-mercaptoethanol). Assays were carried out in triplicate using the chromogenic substrate O-nitrophenyl-β-ᴅ-galactopyranoside (ONPG) according to the method described by Miller [14]. The activity was expressed in Miller units [1000 x $((1.75 \times OD_{550}) - OD_{420})/OD_{600}$ x t x V/mg protein].

ROS determination

In general, aerobically- and anaerobically-generated ROS were assessed using the oxidation-sensitive probe 2′,7′-dihydrodichlorofluorescein diacetate [38]. Briefly, cells grown aerobically or anaerobically in LB medium to $OD_{600nm} \sim 0.4$ were exposed for 15 min to $HAuCl_4$ (250; 125 or 62.5 µM) or to K_2TeO_3 (2 µM). Then, cultures were centrifuged, washed with 50 mM potassium phosphate buffer pH 7.0 and incubated for 30 min in the same buffer containing the probe in the dark (40 µM final concentration) to 37 °C. Cells were subsequently washed and pellets suspended with 1 mL of the same buffer; fluorescence intensity was determined in a multi-well plate reader (TECAN Infinite® M200 Pro) using excitation and

emission wavelengths of 490 and 527 nm, respectively. Emission values were normalized by the optical density at 600_{nm}.

Superoxide generation was assessed as follows. *E. coli* was grown for 30 min as above. After centrifuging and washing with 50 mM potassium phosphate buffer pH 7.0 and incubating in the dark for 15 min with 40 µM dihydroethidine (DHE) to 37 °C, cells were washed, pellets suspended with 1 mL of the same buffer and fluorescence intensity determined using 200 µL of the culture in a multi-well plate reader (TECAN Infinite® M200 Pro, excitation 490_{nm}, emission 625 nm). Emission values were normalized as above.

Determination of reduced thiol concentration

To quantify intracellular thiol content, overnight grown *E. coli* cultures (aerobically or anaerobically) were diluted 1:100 with LB medium and incubated at 37 °C with shaking at 150 rpm to $OD_{600nm} \sim 0.5$. Then, were treated with $HAuCl_4$ (250; 125 or 62.5 µM) or K_2TeO_3 (2 µM); 500 µL aliquots were taken after 15 min and centrifuged at $10,000 \times g$ for 5 min. Sediments were suspended in 1 mL of a solution that contained 5 mM EDTA, 0.1% SDS, 0.1 mM DTNB and 50 mM Tris–HCl buffer pH 8.0. The suspension was incubated for 30 min at 37 °C and subsequently centrifuged at $10,000 \times g$ for 10 min. Supernatants were recovered and the absorbance at 412 nm was determined in a multi-well plate reader. RSH concentration (µM) was calculated using calibration curves constructed with GSH standards (0–200 µM). RSH values were normalized by the protein concentration.

In vivo and in vitro synthesis of gold nanostructures

For synthesizing gold nanostructures in vivo, *E. coli* were grown to exponential phase ($OD_{600nm} \sim 0.5$), treated with ¼ of the Au^{3+} MIC, incubated for 4 h and centrifuged at $9000 \times g$ for 10 min. The bacterial pellet was observed by Transmission Electron Microscopy (TEM) in a Philips Tecnai 12 Bio Doble TEM equipment operating at 200 kV as described by Correa-Llantén et al. [44].

Formation of AuNS in vitro was carried out using cell-free extracts (in 20 mM phosphate buffer containing 100 µg/mL of protein) and incubated overnight with 1 mM $HAuCl_4$ and NADH at 37 °C. AuNS were collected by centrifugation and washed 3 times with sterile water for 10 min at $5000 \times g$ and stored at 4 °C. AuNS were visualized by TEM.

Data analysis

Statistical analysis and graphs were carried out using GraphPad Prism 6.0 (GraphPad Software, Inc.). The confidence interval in the analysis of variance (ANOVA) was set at $p < 0.05$. The statistical significance was

Muñoz-Villagrán *et al. Biol Res*   (2020) 53:26

Page 8 of 9

indicated as follows: $*p < 0.05$, $**p < 0.01$, $***p < 0.001$ and $****p < 0.0001$; *ns* not significant.

Supplementary information

Additional file 1: Figure S1. HAuCl$_4$ susceptibility of *E. coli* grown under anaerobic conditions. **a** *E. coli* growth anaerobically in the presence of the indicated Au^{3+} concentrations. **b** Relationship of the area under the curve (AUC) and HAuCl$_4$ concentration.

Additional file 2: Figure S2. Viability of *E. coli* exposed to Au^{3+} with pretreatments of ROS scavengers. Cells grown to OD$_{600}$ 0.4 were incubated for 30 min in the absence and presence of 2,2 bipyridyl and ascorbic acid, washed and incubated with 0.2 mM Au^{3+} for 15 min. The letters indicate the significance of the one-way statistical analysis ANOVA Multiple comparisons. $****p < 0.0001$, $**p < 0.05$; *ns* not significant.

Abbreviations
AuNS: Nanostructures; ROS: Reactive oxygen species; MIC: Minimal inhibitory concentration; GSH: Glutathione; NS: Nanostructures; AUC: Area under the curve; SDS: Sodium dodecyl sulfate; ONPG: O-nitrophenyl-β-ᴅ-galactopyranoside; DHE: Dihydroethidine; RSH: Intracellular thiol.

Authors' contributions
Conceived and designed the experiments: CM, FC, CR, JR, CV and FA. Performed the experiments: CM, FC, MF, DV, FC, RL and CR. Analyzed the data: CM, FC, RL, DV, CR, JR, CV and FA. Contributed reagents/materials/analysis tools: CV and FA. Wrote the paper: CM, JR, CV, and FA. All authors read and approved the final manuscript.

Availability of data and materials
All data generated or analyzed during this study are included in this published article.

Ethics approval and consent to participate
Not applicable.

Consent for publication
Not applicable.

Competing interests
The authors declare that they have no competing interests.

Author details
[1] Laboratorio Microbiología Molecular, Departamento de Biología, Facultad de Química y Biología, Universidad de Santiago de Chile, Santiago, Chile. [2] Laboratorio de Microbiología Aplicada, Departamento de Ciencias Básicas, Facultad de Ciencias, Universidad Santo Tomás, Sede Santiago, Chile. [3] Laboratorio de Biología estructural, Centro de Genómica y Bioinformática, Universidad Mayor, Santiago, Chile.

References
1. Nies DH. Microbial heavy-metal resistance. Appl Microbiol Biotechnol. 1999;51(6):730–50. https://doi.org/10.1007/s00253005.
2. Lemire JA, Harrison JJ, Turner RJ. Antimicrobial activity of metals: mechanisms, molecular targets and applications. Nat Rev Microbiol. 2013;11(6):371–84. https://doi.org/10.1038/nrmicro3028.
3. Gadd GM. Metals and microorganisms: a problem of definition. FEMS Microbiol Lett. 1992;100(1–3):197–203. https://doi.org/10.1111/j.1574-6968.1992.tb14040.x.
4. Kreuter J. Nanoparticles–a historical perspective. Int J Pharm. 2007;331(1):1–10. https://doi.org/10.1016/j.ijpharm.2006.10.021.
5. Vimbela GV, Ngo SM, Fraze C, et al. Antibacterial properties and toxicity from metallic nanomaterials. Int J Nanomed. 2017;12:3941–65. https://doi.org/10.2147/IJN.S183907.
6. Kumura T, Nishioka H. Intracellular generation of superoxide by copper sulphate in *Escherichia coli*. Mutat Res. 1997;389:237–42.
7. Ackerley DF, Barak Y, Lynch SV, et al. Effect of chromate stress on *Escherichia coli* K-12. J Bacteriol. 2006;188:3371–81. https://doi.org/10.1128/JB.188.9.3371-3381.2006.
8. Pérez JM, Calderón IL, Arenas FA, et al. Bacterial toxicity of potassium tellurite: unveiling an ancient enigma. PLoS ONE. 2007;2:e211. https://doi.org/10.1371/journal.pone.0000211.
9. Park HJ, Kim JY, Kim J, et al. Silver-ion-mediated reactive oxygen species generation affecting bacterial activity. Water Res. 2009;43:1027–32. https://doi.org/10.1016/j.watres.2008.12.002.
10. Barras F, Fontecave M. Cobalt stress in *Escherichia coli* and *Salmonella enterica*: molecular bases for toxicity and resistance. Metallomics. 2011;3:1130–4. https://doi.org/10.1039/c1mt00099c.
11. Imlay JA. Diagnosing oxidative stress in bacteria: not as easy as you might think. Curr Opin Microbiol. 2015;24:124–31. https://doi.org/10.1016/j.mib.2015.01.004.
12. Nam SH, Lee WM, Shin YJ, et al. Derivation of guideline values for gold (III) ion toxicity limits to protect aquatic ecosystems. Water Res. 2014;48:126–36. https://doi.org/10.1016/jwatres.2013.09.019.
13. Lo KKW. Luminescent and photoactive transition metal complexes as biomolecular probes and cellular reagents (Vol. 165). Berlin: Springer; 2015. ISBN 978-3-662-46718-3.
14. Miller JH (1972) Experiments in Molecular Genetics, Cold Spring Harbor Laboratory Press, New York, pp. 201–205, 352–355; 431–433.
15. Zammit CM, Weiland F, Brugger J, et al. Proteomic responses to gold(III)-toxicity in the bacterium *Cupriavidus metallidurans* CH34. Metallomics. 2016;8(11):1204–16. https://doi.org/10.1039/c6mt00142d.
16. Reith F, Etschmann B, Grosse C, et al. Mechanisms of gold biomineralization in the bacterium *Cupriavidus metallidurans*. Proc Natl Acad Sci USA. 2009;106(42):17757–62. https://doi.org/10.1073/pnas.0904583106.
17. Zhang L, Wu L, Si Y, et al. Size-dependent cytotoxicity of silver nanoparticles to *Azotobacter vinelandii*: growth inhibition, cell injury, oxidative stress and internalization. PLoS ONE. 2018;13(12):e0209020. https://doi.org/10.1371/journal.pone.0209020.
18. Li X, Robinson SM, Gupta A, et al. Functional gold nanoparticles as potent antimicrobial agents against multi-drug-resistant bacteria. ACS Nano. 2014;8(10):10682–6. https://doi.org/10.1021/nn5042625.
19. Jones N, Ray B, Ranjit KT, Manna AC. Antibacterial activity of ZnO nanoparticle suspensions on a broad spectrum of microorganisms. FEMS Microbiol Lett. 2008;379:71–6. https://doi.org/10.1111/j.1574-6968.2007.01012.x.
20. Kumari J, Kumar D, Mathur A, et al. Cytotoxicity of TiO2 nanoparticles towards freshwater sediment microorganisms at low exposure concentrations. Environ Res. 2014;1(135):333–45. https://doi.org/10.1016/j.envres.2014.09.025.
21. Cui Y, Zhao Y, Tian Y, et al. The molecular mechanism of action of bactericidal gold nanoparticles on *Escherichia coli*. Biomaterials. 2012;33(7):2327–33. https://doi.org/10.1016/j.biomaterials.2011.11.057.
22. Itoh M, Nakamura M, Suzuki T, et al. Mechanism of chromium (VI) toxicity in *Escherichia coli*: is hydrogen peroxide essential in Cr(VI) toxicity? J

Muñoz-Villagrán *et al. Biol Res*   (2020) 53:26

Page 9 of 9

Biochem. 1995;117(4):780–6. https://doi.org/10.1093/oxfordjournals.jbchem.a124776.

23. Parvatiyar K, Alsabbagh EM, Ochsner UA, et al. Global analysis of cellular factors and responses involved in *Pseudomonas aeruginosa* resistance to arsenite. J Bacteriol. 2005;187(4):4853–64. https://doi.org/10.1128/JB.187.14.4853-4864.2005.

24. Goswami M, Mangoli SH, Jawali N. Involvement of reactive oxygen species in the action of ciprofloxacin against *Escherichia coli*. Antimicrob Agents Chemother. 2006;50(3):949–54. https://doi.org/10.1128/AAC.50.3.949-954.2006.

25. Kohanski MA, Dwyer DJ, Hayete B, et al. A common mechanism of cellular death induced by bactericidal antibiotics. Cell. 2007;130(5):797–810. https://doi.org/10.1016/j.cell.2007.06.049.

26. Borsetti F, Tremaroli V, Michelacci F, et al. Tellurite effects on *Rhodobacter capsulatus* cell viability and superoxide dismutase activity under oxidative stress conditions. Res Microbiol. 2005;156(7):807–13. https://doi.org/10.1016/j.resmic.2005.03.011.

27. Arenas FA, Covarrubias PC, Sandoval JM, et al. The *Escherichia coli* BtuE protein functions as a resistance determinant against reactive oxygen species. PLoS ONE. 2011;6(1):e15979. https://doi.org/10.1371/journal.pone.0015979.

28. Kachur AV, Koch CJ, Biaglow JE. Mechanism of copper-catalyzed oxidation of glutathione. Free Radical Res. 1998;28:259–69. https://doi.org/10.3109/10715769809069278.

29. Turner RJ, Aharonowitz Y, Weiner JH, et al. Glutathione is a target in tellurite toxicity and is protected by tellurite resistance determinants in *Escherichia coli*. Can J Microbiol. 2001;47(1):33–40. https://doi.org/10.1139/cjm-47-1-33.

30. Morales EH, Pinto CA, Luraschi R, et al. Accumulation of heme biosynthetic intermediates contributes to the antibacterial action of the metalloid tellurite. Nat Commun. 2017;8:15320. https://doi.org/10.1038/ncomms15320.

31. Shah M, Badwaik V, Kherde Y, et al. Gold nanoparticles: various methods of synthesis and antibacterial applications. Front Biosci. 2014;19:1320–4. https://doi.org/10.2741/4284.

32. Cabuzu D, Cirja A, Puiu R, et al. Biomedical applications of gold nanoparticles. Curr Top Med Chem. 2015;15(16):1605–13. https://doi.org/10.2174/1568026615666150414144750.

33. Connor DM, Broome AM. Gold nanoparticles for the delivery of cancer therapeutics. Adv Cancer Res. 2018;139:163–84. https://doi.org/10.1016/bs.acr.2018.05.001.

34. Koziol S, Zagulski M, Bilinski T, et al. Antioxidants protect the yeast *Saccharomyces cerevisiae* against hypertonic stress. Free Radic Res. 2005;39(4):365–71. https://doi.org/10.1080/10715760500045855.

35. Luty-Blocho M, Wojnicki M, Fitzner K. Gold nanoparticles formation via Au(III) complex ions reduction with L-ascorbic acid. Int J Chem Kinet. 2017;9(11):789–97. https://doi.org/10.1002/kin21115.

36. Marcon G, Carotti S, Coronnello M, et al. Gold(III) complexes with bipyridyl ligands: solution chemistry, cytotoxicity, and DNA binding properties. J Med Chem. 2002;45:1672–7. https://doi.org/10.1021/jm01997w.

37. Cinellu MA, Zucca A, Stoccoro S, et al. Synthesis and characterization of gold(III) adducts and cyclometallated derivates with 6-benzyl- and 6-alkyl-2,2´-bipyridines. J Chem Soc. 1996;22:4217–25. https://doi.org/10.1039/dt9960004217.

38. Royall JA, Ischiropoulos H. Evaluation of 2´,7´-dichlorofluorescein and dihydrorhodamine 123 as fluorescent probes for intracellular H_2O_2 in cultured endothelial cells. Arch Biochem Biophys. 1993;302:348–55. https://doi.org/10.1006/abbi.1993.1222.

39. Chen J, Rogers SC, Kavdia M. Analysis of kinetics of dihydroethidium fluorescence with superoxide using xanthine oxidase and hypoxanthine assay. Ann Biomed Eng. 2013;41(2):327–37. https://doi.org/10.1007/s10439-012-0653-x.

40. Greenberg JT, Monach P, Chou JH, et al. Positive control of a global antioxidant defense regulon activated by superoxide-generating agents in *Escherichia coli*. Proc Natl Acad Sci USA. 1990;87:6181–5. https://doi.org/10.1073/pnas.87.16.6181.

41. Chian SM, Schellhorn HE. Regulators of oxidative stress response genes in *Escherichia coli* and their functional conservation in bacteria. Arch Biochem Biophys. 2012;525(2):161–9. https://doi.org/10.1016/j.abb.2012.02.007.

42. Masip L, Veeravalli K, Georgiou G. The many faces of glutathione in bacteria. Antioxid Redox Signal. 2006;8(5–6):753–62. https://doi.org/10.1089/ars.2006.8.753.

43. Bird LJ, Coleman ML, Newman DK. Iron and copper act synergistically to delay anaerobic growth of bacteria. Appl Environ Microbiol. 2013;79(12):3617–27. https://doi.org/10.1128/AEM.03944-12.

44. Correa-Llantén D, Muñoz-Ibacache S, Castro M, et al. Gold nanoparticles synthesized by *Geobacillus* sp. strain ID17 a thermophilic bacterium isolated from Deception Island Antarctica. Microbial Cell Fact. 2013;12:75. https://doi.org/10.1186/1475-2859-12-75.

45. Narayanan KB, Sakthivel N. Biological synthesis of metal nanoparticles by microbes. Adv Colloid Interface Sci. 2010;156:1–13. https://doi.org/10.1016/j.cis.2010.02.001.

46. Thakkar K, Mhatre S, Parikh R. Biological synthesis of metallic nanoparticles. Nanomedicine. 2010;23:257–62. https://doi.org/10.1016/j.nano.2009.07.002.

47. Figueroa M, Fernández V, Arenas M, et al. Synthesis and antibacterial activity of metal(loid) nanostructures by environmental multi-metal(loid) resistant bacterial and metal(loid)-reducing flavoproteins. Front Microbiol. 2018;9:959. https://doi.org/10.3389/fmicb.2018.00959.

48. Sambrook J, Russell D. Molecular cloning. A laboratory manual. 3rd ed. Cold Spring Harbor: Cold Spring Harbor Laboratory Press; 2001.

49. Arenas FA, Díaz WA, Leal CA, et al. The *Escherichia coli btuE* gene, encodes a glutathione peroxidase that is induced under oxidative stress conditions. Biochem Biophys Res Commun. 2010;398:690–4. https://doi.org/10.1016/j.bbrc.2010.07.002.

50. Bhowmick AR, Chattopadhyay G, Bhattacharya S. Simultaneous identification of growth law and estimation of its rate parameter for biological growth data: a new approach. J Biol Phys. 2014;40(1):71–95. https://doi.org/10.1007/s10867-013-9336-6.

51. Peleg M, Corradini MG, Normand MD. The logistic (Verhulst) model for sigmoid microbial growth curves revisited. Food Res Int. 2007;40(7):808–18. https://doi.org/10.1016/j.foodres.2007.01.012.

52. Sprouffske K, Wagner A. Growthcurver: an R package for obtaining interpretable metrics from microbial growth curves. BMC Bioinform. 2016;17:172. https://doi.org/10.1186/s12859-016-1016-7.

53. Contreras F, Vargas E, Jimenez K, et al. Reduction of gold (III) and tellurium (IV) by *Enterobacter cloacae* MF01 results in nanostructure formation both in aerobic and anaerobic conditions. Front Microbiol. 2018;9:3118. https://doi.org/10.3389/fmicb.2018.03118.

Publisher's Note